Boundary Value Effects on Migration Patterns in Hydraulically Fractured Shale Formations

Toyin C. Aseeperi[1]

[1]Ralph. E Martin Department of Chemical Engineering, University of Arkansas, Fayetteville

*Corresponding author: 2215 Bell Engineering, University of Arkansas, Fayetteville, 72701
taseeper@uark.edu

Abstract: In the design of models to optimize the production of gas from shale reservoirs, the formation boundaries are usually assumed to be sufficiently impermeable as to be treated as a no-flux boundary. However, during hydraulic fracturing, there can be re-activation of closed/sealed faults and natural fractures in the formation, which may lead to changes in the boundary conditions. This project seeks to investigate this scenario.

For computational tractability, the simulation domain is sized around a production stage. A novel approach to modeling the fractures in the formation by making use of semi-explicit representations of horizontal bedding planes and hydraulic fractures is implemented in this study. The boundary conditions and the effects of the changing permeability in the domain are varied. The flow equation is solved using COMSOL Multiphysics 4.4

This work presents the results of a numerical simulation of gas flow in fractured shale gas reservoirs. Our results indicate that the assumption of a no-flux boundary condition in the presence of a fault along the formation boundary, leads to an over prediction of wellbore gas production values and a non-accounting of the leak-off values that may be associated with any faults across the boundary.

Keywords: Shale gas production, fracture re-activation, Semi-explicit fracture representation, Boundary effects.

1. Introduction

Natural gas in shale reservoirs is believed to be stored as free gas in both shale matrix and natural fracture system, and as adsorbed gas on the surface of shale matrix. These different storage mechanisms affect the speed and efficiency of gas production(Song 2010; IEA 2012). Flow in the reservoir is usually termed Dual-Permeability with the natural fractures and the tight matrix serving as the different permeability pathways through which fluid recovery from the reservoir is achieved. However, since the matrix is typically a very low permeability rock, and most of the natural fractures have been sealed-in under high pressure compaction of the source rock, practical exploitation of the reservoir is only achievable after it has been hydraulically fractured.

Research and development into the geological controls and production technologies-particularly the techniques of horizontal drilling and hydraulic fracturing during the past several decades has enabled operators in the USA to begin to unlock the vast potential associated with these resources. There has been a remarkable increase in shale gas development and production activities using the hydraulic fracturing process. This in turn has resulted in significant amount of public concern about the environmental effects of the technology.

A frequently expressed concern about shale gas development is that during hydraulic fracturing operations in deep shale, developers do not have complete control over fracture location; therefore methane, contaminants naturally occurring in formation water, and fracturing fluids may migrate from the target formation into aquifers and drinking water supplies.(Rao 2012; US DOE 2009) Concerns about potential free gas migration beyond the boundaries of the reservoir however seem to be a more pressing issue in recent times. This concern is justified by the fact that the gas phase migrates much faster than the liquid phase in porous formations and this movement can be further enhanced by the presence of fractures, as flow in fractures is known to be orders of magnitude faster than flow in the porous matrix.

To ensure that gas recovery from unconventional reservoirs is optimized and

carried out in an environmentally safe manner, a better understanding of the fluid flow behavior and reservoir dynamics in the shale formation is essential.

Flow modeling in fractured rocks can be difficult to observe and characterize. This is because only a trace of the fracture can be observed in cases where the whole geometry of the fracture isn't hidden in the subsurface. To embark on a study of the fractured rock therefore, the fractured system needs to be represented by an appropriate conceptual model. The classical description of a hydraulic fracture is a single bi-wing planar crack with the wellbore at the center of two wings. However, almost all physical fracture verifications performed have proven this description to be oversimplified. (Gorocu 2010; Osholake 2010; C. Wang and Wu 2014). In the hydraulic fracturing of deviated wells, fractures sometimes reorient and interact with natural bedding planes and other fractures as they propagate. A fracture treatment in a tight shale formation is therefore more likely to generate complex fracture geometries which are difficult to characterize, due to interactions with natural fractures. Numerical simulations are thus employed to evaluate and predict the extent, location and direction of these fractures (Carter, 2010, Fisher, 2002).

In the past decade, there has been an increased drive towards research aimed at identifying and understanding the complicated flow behaviors and physics associated with shale-gas flow modeling (Cipolla et al. 2009; Li et al. 2013; Leahy-Dios et al. 2011; X. Wang and Ghassemi 2012; Ding et al. 2014) , however the number of studies and effective reservoir simulators that are currently available are still relatively small. These models are generally intended to study conditions for optimized gas recovery from the reservoir to the wellbore, and so the formation boundaries are assumed to be sufficiently impermeable as to be treated as a no-flux barrier to fluid movement out of the formation. However, during the hydraulic fracturing process, re-activation of sealed faults that extend beyond the reservoir boundaries and natural fractures at the formation boundary sometimes occur. When this occurs, a no-flux boundary can no longer be specified at that boundary of the domain, and this study seeks to study the effect of this change on the flux out of the formation.

2. Governing Equations

The mathematical equations that describe fluid flow and transport processes in porous media may be developed from the fundamental principle of conservation of mass of fluid or of solute and Newton's second law of motion (Lapcevic et al, 2006).

A simplified statement of the laws is presented below:

$$v = -\frac{k}{\mu}\nabla p \qquad (1)$$

$$\frac{\partial \rho}{\partial t} + \nabla.(\rho v) = 0 \qquad (2)$$

where v is the velocity of the fluid in the formation, k is the permeability of the rock, ρ is the fluid density, μ is the fluid viscosity, ∇p is the pressure gradient, and the term $\frac{\partial \rho}{\partial t}$ represents the rate of change in mass in the control volume.

Depending on if the formation been studied is a dry-gas reservoir or one with significant water content, a single phase or two-phase flow model is considered as the conceptual flow model for in shale, however, since we are most concerned with the migration pattern of the gas in the formation, we assume that the water in our system is at residual saturation and immobile. This reduces our flow model to a single phase flow formulation.

This single flow equation can be specified in two ways:

a. Without accounting for the adsorbed phase- as specified in (3a)
b. Accounting for desorption of adsorbed gas- equation (3b)

$$\frac{\partial}{\partial t}\big(M_p\big) = -\nabla.(\rho v) \qquad (3a)$$

$$\frac{\partial}{\partial t}\big(M_s + M_p\big) = -\nabla.(\rho v) \qquad (3b)$$

where M_s represents the amount of mass present in the adsorbed state and M_p is the amount of gas present in the pores in the formation.

To account for the adsorbed gas within the solid phase of the rock, the mass conservation equation is modified as shown in equation (3b). The mass of adsorbed gas in the formation can be expressed by the relationship in equation (4)

$$M_s = \rho_k \rho_g V_{ads} \tag{4}$$

where ρ_k is the bulk density of the rock, ρ_g is the gas density at standard conditions and V_{ads} is the volume of adsorbed gas. V_{ads} is specified by making use of the Langmuir adsorption isotherm function(Leahy-Dios et al. 2011; Wu et al. 2013).

The Langmuir isotherm gives the dependency of the adsorbed gas volume on the reservoir pressure at any point in time. The relationship is stated as

$$V_{ads} = \frac{P}{P + P_L} V_L \tag{5}$$

where P is the reservoir pressure, P_L is the pressure at which 50% of the gas is desorbed and is referred to as the Langmuir pressure and V_L is the gas content, which is also known as the Langmuir volume and is specified in scf/ton. Thus we can rewrite equation (4) as

$$M_s = \rho_k \rho_g \frac{P}{P + P_L} V_L \tag{6}$$

$$\frac{\partial}{\partial t}(M_s) = \frac{\partial}{\partial t}(\rho_k \rho_g \frac{P}{P + P_L} V_L) \tag{7}$$

$$= \rho_k \rho_g \frac{\partial V_{ads}}{\partial P} \frac{\partial P}{\partial t} \tag{8}$$

$$\frac{\partial V_{ads}}{\partial P} = \frac{V_L * P_L}{(P + P_L)^2} \tag{9}$$

Therefore

$$\frac{\partial}{\partial t}(M_s) = \rho_g \frac{V_L * P_L * \rho_k}{(P + P_L)^2} \frac{\partial P}{\partial t} \tag{10}$$

The mass of gas in the reservoir pore volume can be expressed as a function of the porosity of the reservoir and the density of the fluid in the reservoir. i.e.

$$M_p = \rho_g \theta \tag{11}$$

where θ is the porosity of the reservoir.

$$\frac{\partial}{\partial t}(M_p) = \frac{\partial}{\partial t}(\rho_g \theta) \tag{12}$$

$$= \theta \frac{\partial \rho}{\partial P} \frac{\partial P}{\partial t} \tag{13}$$

The isothermal compressibility of a gas C_f is defined as $\frac{1}{\rho} \frac{\partial \rho}{\partial P}$ so that

$$\frac{\partial \rho}{\partial P} = \rho_g C_f \tag{14}$$

and

$$\frac{\partial}{\partial t}(M_p) = \rho_g C_f \theta \frac{\partial P}{\partial t} \tag{15}$$

therefore

$$\frac{\partial}{\partial t}(M_s + M_p) = \rho_g \frac{V_L * P_L * \rho_k}{(P + P_L)^2} \frac{\partial P}{\partial t} + \rho_g C_f \theta \frac{\partial P}{\partial t} \tag{16}$$

Re-writing equation 3a and 3b in the expanded form gives

$$\rho_g \frac{\partial P}{\partial t}(C_f \theta) = -\nabla.(\rho v) \tag{17a}$$

$$\rho_g \frac{\partial P}{\partial t}\left(\frac{V_L * P_L * \rho_k}{(P + P_L)^2} + C_f \theta\right) = -\nabla.(\rho v) \tag{17b}$$

which specifies the governing equation for fluid flow in shale.

3. Description of Numerical Model

The development of predictive models for flow and transport in shale formations is still an active area of research. While reservoir production rates and completion data are becoming available for the validation of deterministic models, the number of reservoir parameters with inherent uncertainties are still sizeable enough, that the use of synthetic models based on available information forms the basis for most studies.

Completion methods in shale gas formations involves inducing hydraulic fractures into a naturally fractured domain (See **Figure 1**). Most models in literature (Cipolla et al. 2009; Rubin 2010; Li et al. 2013; Ding et al. 2014) make use of the conventional orthogonal transverse fractures as a way to account for natural fracture in the formation. However shale formations have

been observed to be made up of mostly horizontal layers of laminated bedrock. It therefore seems that a suitable conceptual model for a shale reservoir should have horizontal fracturing network elements (bedding planes) built into the simulation.

In this study, we present a hybrid approach to modeling shale reservoirs by making use of a single porosity model with semi-explicit representations of horizontal bedding planes and hydraulic fractures.
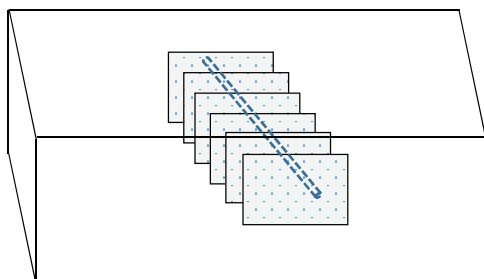

Figure. 1—Schematic of a typical completion arrangement in shale gas production sites which makes use of transverse fractures in a horizontal well.

A conceptual model is set up based on published average reservoir data for a producing shale formation(C. Wang, Ding, and Wu 2013) and published well completion data (Harpel et al. 2012; Ramakrishnan et al. 2011). The detailed list of the reservoir and hydraulic fracture parameters used for the simulation is presented in **Table 1**. For computational tractability the model is sized around one production stage with 2 foot perforated sections located at 80 foot intervals.

The following assumptions are implemented in our study:

i. The formation is homogenous and rectangular.
ii. The formation is completed using multiple transverse fractures originating at perforations and intersecting the horizontal well.
iii. The hydraulic fractures fully penetrate the formation.
iv. The boundaries of the formation are considered to be impermeable, except in the case where it intersects a pre-existing fault or fracture –in which case a pressure boundary condition is specified.

v. The effects of desorption are not modeled in this study.
vi. Gas in the reservoir flows into the wellbore only through the perforated intervals.

Table 1—Model Input Parameters

Parameter	Value	Units
Matrix permeability	1.0×10^{-4}	mD
Porosity of the matrix	5	%
Initial Reservoir pressure	3800	psi
Well-bore pressure	500	psi
Well-bore radius	0.25	ft
Reservoir thickness	250	ft
Reservoir width	2000	ft
Reservoir length	500	ft
Number of fractures	6	
Number of bedding planes	2	
Hydraulic fracture spacing	82	ft
Hydraulic fracture length	1.0×10^{5}	mD
Hydraulic fracture porosity	50	%
Hydraulic fracture length	500	ft
Hydraulic fracture height	250	ft
Bedding plane permeability	2.0×10^{3}	mD
Bedding plane porosity	50	%
Bedding plane length	1950	ft
Bedding plane depth	495	ft
Fracture/Fault Aperture	0.02	ft
Fault permeability	2.0×10^{3}	mD
Fault length	495	ft
Fault width	20	ft
Fluid Viscosity	0.0184	cP
Fluid Density	0.66	kg/m^3
Fluid compressibility	2.5×10^{-4}	psi^{-1}

4. Use of COMSOL Multiphysics

The solution to the flow equations was obtained using the Subsurface Flow Module of COMSOL Multiphysics 4.4. The flow in the domain was specified using the Darcy's Law interface which combines equation (3a) with the continuity equation as described in the equation section. Flow through the fractures is modeled using

COMSOL's Semi-Explicit Fracture Flow Boundary condition. The fracture flow interface uses the tangential version of Darcy's law. It increases the computational efficiency of the simulation as it makes use of a reduced dimensionality for the fracture domain, i.e. a 3D fully explicit fracture is modeled as a 2D planar geometry. The collapsed dimension is accounted for in a re-formulated equation for flow (equation (10)), which makes use of tangential derivatives to the pressure gradient to solve for pressure distribution within the fracture.

$$q_f = -\frac{k_f}{\mu} d_f (\nabla_T p) \qquad (10)$$

Here q_f is the volume flow rate per unit length in the fracture, k_f is the fracture's permeability, μ is the fluid dynamic viscosity, d_f is the thickness of the fracture, ∇_T denotes the gradient operator restricted to the fracture's tangential plane and p is the pressure.

5. Results & Discussion

The results presented in this section are based on the comparison of three different reservoir states shown in Figure 2 below:

I. The formation with no natural bedding planes and a pre-existing fault (Pre-frac 1).

II. The formation with natural bedding planes and a pre-existing fault (Pre-frac 2)

III. Hydraulically fractured formation with natural bedding planes and pre-existing fault (Post-frac).

The simulations were conducted using the no-flux boundary conditions as a base case and subsequently revising the boundary conditions at the edge of the fault to incorporate the pressure changes associated with time.
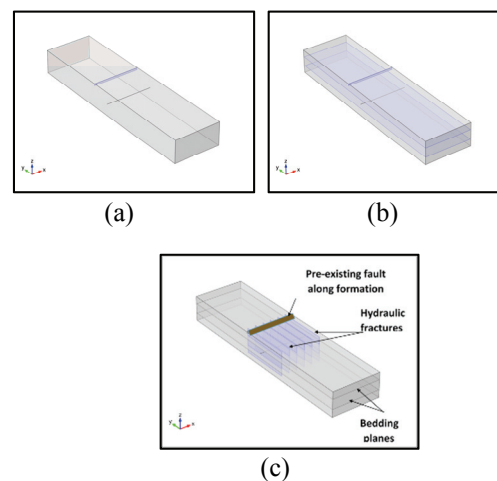

(a)   (b)

(c)

Figure. 2—Reservoir geometry showing Pre-fracturing states (a) and (b), and Post-fracturing state (c) utilized for simulations

In **Figures 3(a), 4(a)**, and **5(a),** the pressure distribution on the cross-section of the reservoir through the fault boundary for conceptual models I, II and III after a 1-year period is presented. There is no significant pressure dissipation from the initial reservoir condition for cases I and II. In contrast, Figure 5(a) shows a marked pressure dissipation in the formation, which can be attributed to the network of interconnected fractures made available by the hydraulic fracturing process.
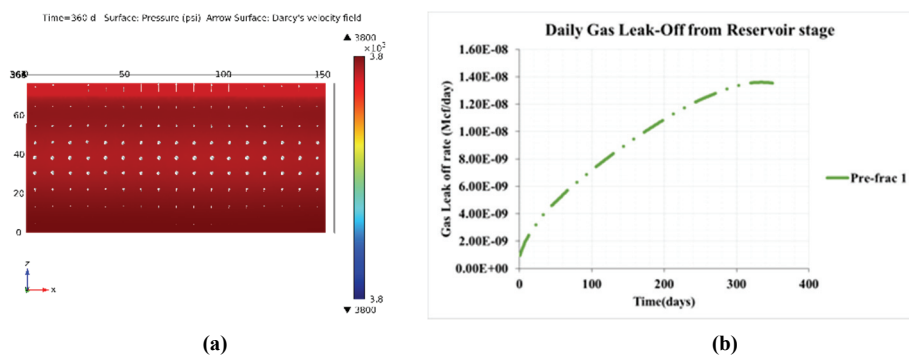

(a)   (b)

Figure. 3— **Conceptual Model I - Pre-frac1 (a)** Pressure distribution and Arrow surface plots for cut-plane sections through plane containing boundary fault **(b)** Predicted leak-off rates at the fault boundary.
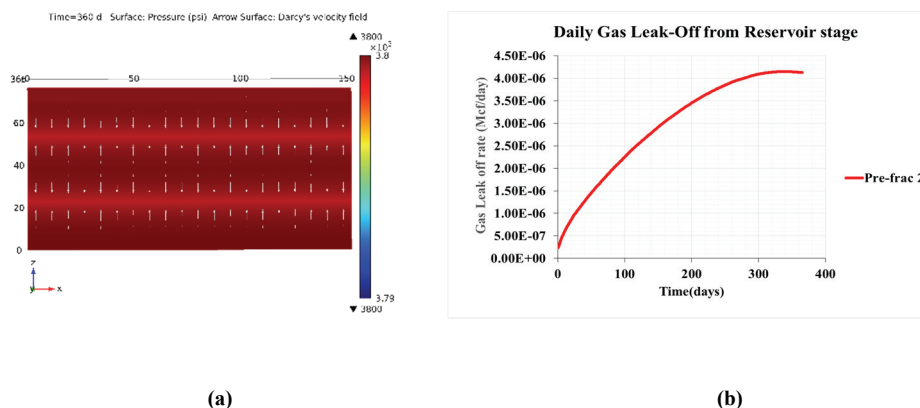
(a)

(b)

Figure. 4— Conceptual Model II - Pre-frac2 (a) Pressure distribution and Arrow surface plots for cut-plane sections through plane containing boundary fault **(b)** Predicted leak-off rates at the fault boundary.
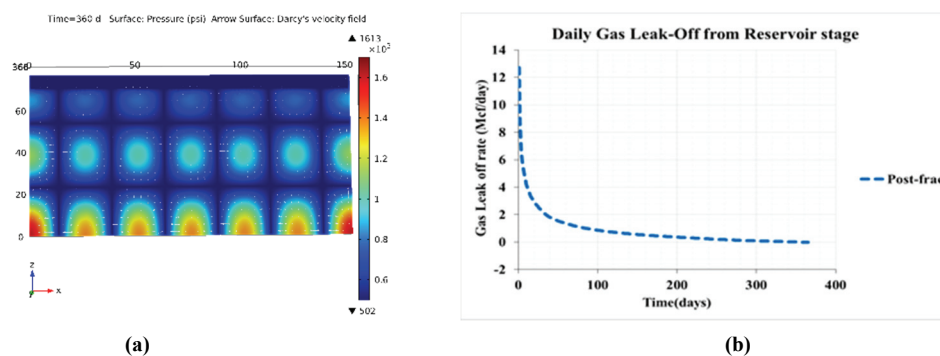

(a)

(b)

Figure. 5— Conceptual Model III – Post-Frac (a) Pressure distribution and Arrow surface plots for cut-plane sections through plane containing boundary fault **(b)** Predicted leak-off rates at the fault boundary.

The arrow surface plots show the direction of fluid migration in the plane boundary. Flow directions in the fault which is located in the top 20ft of the boundary is towards the fault in Pre-frac 1 and towards both the fault and the horizontal fractures in the Pre-frac 2 case, showing that there is fluid movement towards the boundary. This observation can also be explained by the leak-out plots shown in **Figures 3(b) and 4(b)** i.e. the increased rate of the gas leak-off rate in both cases. For the Post-frac case however at the end of the 1 year simulation period, the flow directions are predominantly in the directions of the interconnected networks in the reservoir and not the fault boundary as seen in **Figure 5(a).** Also, the leak-off rate in the Post-frac case-while being initially 8 orders of magnitude higher than values observed in the Pre-frac cases at the start of production, tapers off and becomes relatively constant as can be seen in **Figure 5(b).**
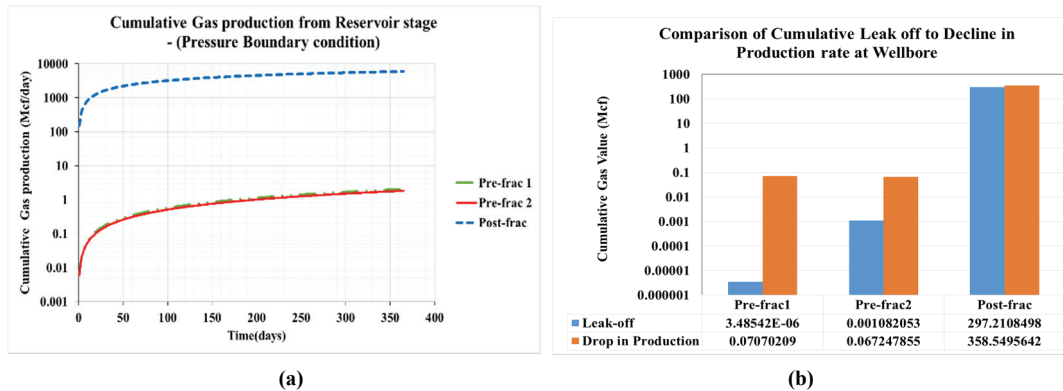
Figure. 6— (a) Comparison of cumulative gas production from the reservoir and **(b)** Comparison of cumulative leak off rates to decline in Wellbore production
- for a 1 year period for the Pre-frac1, Pre-frac 2 and Post frac modeling scenarios.

Figure 6(a) presents a comparison of the gas production values at the wellbore for the three conceptual models after a 1-year period. Our simulated results show that the introduction of hydraulic fractures into the formation leads to a four orders of magnitude difference in the cumulative gas production values. Also the comparison of the value of leak-off at the boundary to the decrease in gas production noticed at the wellbore as a result of the changing the no-flux boundary condition at the fault edge is presented in **Figure 6(b).** In all cases, the presence of the fault at the boundary reduces the amount of gas recovered at the wellbore.

6. Conclusions

Using numerical simulation, we present results that show that the assumption of a no-flux boundary condition in the presence of a fault along the boundary of a formation leads to an over prediction of wellbore gas production values and an improper accounting of the leak-off values that may be associated with the fault across the boundary. While the leak-off values are relatively low before the introduction of fractures into a formation, a cumulative leak off value of about 300Mcf – a value eight orders of magnitude higher than what is predicted in the pre-fracturing state- is the simulated result for the post-fractured formation.

To ascertain that this leak-off stream does not travel into overlying formations and become a contaminant source in gas production areas, further investigations and sensitivity analysis needs to be carried out on the fault parameters, such as its aperture, height and location in the reservoir, as well as on the properties (permeability and bedrock thickness) of the overlying formations.

7. Nomenclature

v - fluid velocity
k - permeability of the rock,
ρ – fluid density
μ - fluid viscosity,
p - pressure
$\frac{\partial \rho}{\partial t}$ - rate of mass change
M_s - mass associated with adsorption
M_p - mass contained in pore spaces.
θ - reservoir porosity
C_f - isothermal compressibility of fluid
q_f - fluid flow rate in the fracture,
k_f - fracture permeability,
d_f - fracture thickness/aperture
∇_T - tangential gradient operator

8. References

Cipolla, Craig, Elyezer Lolon, James Erdle, and Barry Rubin. 2009. "Reservoir Modeling in Shale-Gas Reservoirs." In *Proceedings of the SPE Eastern Regional Meeting*, 19. Charleston, West Virginia: Society of Petroleum Engineers.

Ding, Didier, Yu-Shu Wu, Nicolas Farah, Cong Wang, and Bernard Bourbiaux. 2014. "Numerical Simulation of Low Permeability Unconventional Gas Reservoirs." In *Proceedings of the SPE/EAGE European Unconventional Conference*, 30. Vienna, Austria: Society of Petroleum Engineers.

Harpel, Jennifer, Leonard Barker, Jeremy Fontenot, Christian Carroll, Steve Thomson, and Karen Olson. 2012. "Case History of the Fayetteville Shale Completions." In *Proceedings of the SPE Hydraulic Fracturing Technology Conference*. The Woodlands, Texas: Society of Petroleum Engineers.

IEA. 2012. *Golden Rules for a Golden Age of Gas*. World Energy Outlook Special Report on Unconventional Gas.

Leahy-Dios, Alana, Mita Das, Anshul Agarwal, and Robert D. Kaminsky. 2011. "Modeling of Transport Phenomena and Multicomponent Sorption for Shale Gas and Coalbed Methane in an Unstructured Grid Simulator." In *Proceedings of the SPE Annual Technical Conference*. SPE: Society of Petroleum Engineers.

Li, Chunlou, Randy Lafollette, Andy Sookprasong, and Sharon Wang. 2013. "Characterization of Hydraulic Fracture Geometry in Shale Gas Reservoirs Using Early Production Data." In *Proceedings of the International Petroleum Technology Conference (IPTC)*.

Osholake, Tunde. 2010. "Factors Affecting Hydraulically Fractured Well Performance in the Marcellus Shale Gas Reservoirs." Master's Thesis, State Park, PA: The Pennsylvania State University.

Ramakrishnan, Hariharan, Eva Peza, Shekhar Sinha, Miriam Woods, Chris Ikeocha, Flemming Mengel, Yves Simon, Paul Pearce, Jeff Kiester, and Steven Mcketta. 2011. "Understanding and Predicting Fayetteville Shale Gas Production Through Integrated Seismic-to-Simulation Reservoir Characterization Workflow." In *Proceedings of the SPE Annual Technical Conference and Exhibition*. Denver, Colorado.

Rao, Vikram. 2012. *Shale Gas: The Promise and the Peril*. Research Triangle Park, NC: RTI Press.

Rubin, Barry. 2010. "Accurate Simulation of Non Darcy Flow in Stimulated Fractured Shale Reservoirs." In *Proceedings of the SPE Western Regional Meeting*. Anaheim, California.

Song, Bo. 2010. "Pressure Transient Analysis and Production Analysis for New Albany Shale Gas Wells." College Station: Texas A&M University.

US DOE. 2009. "Modern Shale Gas Development in the United States: A Primer."

Wang, Cong, Didier Ding, and Yu-Shu Wu. 2013. "Characterizing Hydraulic Fractures in Shale Gas Reservoirs Using Transient Pressure Tests." In *Proceedings of the SPE Hydraulic Fracturing Technology Conference*. The Woodlands, Texas.

Wang, Cong, and Yu-Shu Wu. 2014. "Modeling Analysis of Transient Pressure and Flow Behavior at Horizontal Wells with Multi-Stage Hydraulic Fractures in Shale Gas Reservoirs." In *Proceedings of the SPE Unconventional Resources Conference*. Woodlands. Texas.

Wang, Xiaonan, and Ahmad Ghassemi. 2012. "A 3D Thermal-Poroelastic Model for Geothermal Reservoir Stimulation." In *Thirty-Seventh Workshop on Geothermal Reservoir Engineering*. California.

9. Acknowledgements